The Plant Cell, Vol. 9, 1999–2010, November 1997 © 1997 American Society of Plant Physiologists

Pollen Tube Growth and the Intracellular Cytosolic Calcium Gradient Oscillate in Phase while Extracellular Calcium Influx Is Delayed

Terena L. Holdaway-Clarke,[a,1] José A. Feijó,[b] Grant R. Hackett,[a] Joseph G. Kunkel,[a] and Peter K. Hepler[a]

[a]Biology Department, Morrill Science Center, University of Massachusetts, Amherst, Massachusetts 01003
[b]Department Biologia Vegetal, Faculdade de Ciências, Universidade de Lisboa, Campo Grande, Ed.C2. P-1700 Lisbon, Portugal

Ratio images of cytosolic Ca^{2+} (Ca^{2+}_i) in growing, fura-2–dextran–loaded *Lilium longiflorum* pollen tubes taken at 3- to 5-sec intervals showed that the tip-focused $[Ca^{2+}]_i$ gradient oscillates with the same period as growth. Similarly, measurement of the extracellular inward current, using a noninvasive ion-selective vibrating probe, indicated that the tip-directed extracellular Ca^{2+} (Ca^{2+}_o) current also oscillates with the same period as growth. Cross-correlation analysis revealed that whereas the $[Ca^{2+}]_i$ gradient oscillates in phase with growth, the influx of Ca^{2+}_o lags by ~11 sec. Ion influx thus appears to follow growth, with the effect that the rate of growth at a given point determines the magnitude of the ion influx ~11 sec later. To explain the phase delay in the extracellular inward current, there must be a storage of Ca^{2+} for which we consider two possibilities: either the inward current represents the refilling of intracellular stores (capacitative calcium entry), or it represents the binding of the ion within the cell wall domain.

INTRODUCTION

Pollen tube growth is the process that delivers the male gametes to the egg apparatus in flowering plants and thus is essential for sexual reproduction (Heslop-Harrison, 1987; Mascarenhas, 1993; Taylor and Hepler, 1997). Among the most rapidly growing of all cells, the pollen tube may reach rates of several millimeters per hour (Barnabás and Fridvalszky, 1984) and is driven solely through extension at its extreme apex. Calcium ions (Ca^{2+}) are essential for this process, being needed in the culture medium above 10 μM but below 10 mM (Picton and Steer, 1983). The importance of Ca^{2+} to growth is further emphasized by the unique physiological expressions of the ion both intracellularly and extracellularly (Hepler, 1997).

Within the growing pollen tube, free cytosolic Ca^{2+} (Ca^{2+}_i) occurs in a steep tip-focused gradient extending from above 3 μM at the apex of the growing tube to basal levels of 150 to 300 nM within 20 μm (Rathore et al., 1991; Miller et al., 1992; Pierson et al., 1994, 1996). That this gradient is necessary for growth derives from studies showing that inhibition of elongation by a variety of means, including 1,2-*bis*(2-aminophenoxy)ethane-*N*,*N*,*N*′,*N*′-tetraacetic acid (BAPTA) buffer injection, mild thermal shock, and the application of elevated osmoticum, Ca^{2+} channel blockers, or caffeine, leads to a concomitant dissipation of the gradient (Rathore et al., 1991; Pierson et al., 1994; Li et al., 1996). Alternatively, the experimental generation of elevated internal levels of $[Ca^{2+}]_i$ through an apically localized photolysis of caged Ca^{2+} reveals that the direction of growth is determined by the presence and position of the tip-focused gradient (Malhó and Trewavas, 1996). On the outside of the cell, there is similarly polarized expression of extracellular Ca^{2+} (Ca^{2+}_o) in which the ion exhibits a tip-directed influx or inward current (Kühtreiber and Jaffe, 1990; Pierson et al., 1994, 1996). It too appears closely linked to growth because the different conditions, noted above, that block cell elongation and dissipate the intracellular gradient also essentially eliminate the tip-directed Ca^{2+}_o current (Pierson et al., 1994, 1996).

The relationship between $[Ca^{2+}]_i$ and pollen tube elongation has gained additional momentum recently with the discovery that both the intracellular ion levels and the growth rate oscillate (Pierson et al., 1996). In lily pollen tubes, the change can be as much as fourfold, with apical $[Ca^{2+}]_i$ levels oscillating from 700 to >3000 nM, whereas the growth oscillates from 0.1 μm sec^{-1} to 0.38 μm sec^{-1}. Detailed analysis of the growth rate oscillation, especially for pollen tubes longer than 700 μm, showed a very regular 20- to 30-sec period. Although instrumental limitations at the time prevented us from gaining a rapid measurement of the $[Ca^{2+}]_i$ changes, it was clear, nevertheless, from low-resolution analyses that the oscillations of $[Ca^{2+}]_i$ and growth changed together; as $[Ca^{2+}]_i$ increased, so did the growth rate (Pierson et al., 1996).

[1]To whom correspondence should be addressed. E-mail terena@bio.umass.edu; fax 413-545-3243.

These important results have now come under increasingly detailed scrutiny. First, using the photoprotein aequorin, Messerli and Robinson (1997) observed that lily pollen tubes display pulses in $[Ca^{2+}]_i$ at 40-sec intervals. Growth had a similar period; however, it was not possible to directly correlate these two processes and determine the phase relationship. Second, in pollen tubes loaded with the single wavelength indicator Calcium Green–dextran, Messerli and Robinson (1997) improved the time resolution and showed that within 5 sec, the rise in $[Ca^{2+}]_i$ and the increase in growth rate are positively correlated.

Simultaneously, we have also addressed this problem (Hepler et al., 1997) by taking advantage of the superior properties of a ratiometric dye, fura-2–dextran, which permits us to gain both high-resolution spatial and quantitative information that is not possible with Calcium Green when used as a single wavelength indicator (Hepler, 1997). Our results also reveal a close and positive correlation between $[Ca^{2+}]_i$ and growth. However, they provide spatial evidence that the rise in $[Ca^{2+}]_i$ occurs at the extreme apex as well as information on its magnitude. In addition to the $[Ca^{2+}]_i$ gradient, we have also measured the tip-directed Ca^{2+}_o current by using an ion-selective vibrating electrode. We have discovered that the Ca^{2+}_o current oscillates with the same period as does the growth rate; however, it is delayed in phase by ~11 sec. Here, we investigate the phase relationships between oscillations of growth rate, the $[Ca^{2+}]_i$ gradient, and the Ca^{2+}_o current as a means of understanding how growth is regulated in this simplified system.

RESULTS

Simultaneous Measurement of Pollen Tube Growth and the Tip-Focused $[Ca^{2+}]_i$ Gradient

Because growth oscillation occurs within a 20- to 30-sec interval, it was first necessary to accelerate data acquisition, which previously had been limited to ~30 sec between images (Pierson et al., 1996). By modifying our computer and shutter system, we shortened this to 3 to 5 sec in which the process was automated. Growing tubes were loaded with the Ca^{2+}-sensitive ratio dye fura-2–dextran, and sequences up to 30 ratio–pair images were taken every 3 to 5 sec and used to calculate both the growth rate and $[Ca^{2+}]_i$ at the tip. It was necessary to keep the intensity of the excitation illumination as low as possible so that pollen tube growth would not be disrupted; we found that longer exposures with lower light intensity were more favorable than were shorter exposures at higher intensity. All data presented were taken from tubes that continued to grow after a sequence of 20 to 30 ratio images had been collected.

Figure 1A shows dynamic changes in the $[Ca^{2+}]_i$ gradient at the tip of a growing pollen tube and accompanying oscillations in growth rate. Two different media were used in these intracellular investigations: regular growth medium, as used in previous studies (Miller et al., 1992; Pierson et al., 1996), and a modified low-calcium, low-buffer growth medium (LCLB), which was also suitable for use in experiments measuring the Ca^{2+}_o influx at the tip of pollen tubes. Figures 1B and 1C show that for tubes grown in either medium, the period and shape of both growth rate and $[Ca^{2+}]_i$ curves are very similar and are in phase with each other. These tubes displayed growth oscillations with periods that ranged from 15 to 46 sec, in agreement with previous observations (Pierson et al., 1996).

These data have also been plotted as a series of nested curves, as shown in Figure 2, and reveal the spatial characteristics of the $[Ca^{2+}]_i$ profile during the oscillations. From these observations, it is readily apparent that the changes are largely at the extreme apex of the tube, with relatively little change in the shank. Indeed, we purposely explored the possibility that the oscillations might be generating basipetally traveling waves; however, in all of our studies, we were unable to detect a single example. Thus, the rise in $[Ca^{2+}]_i$, which appears to originate from ion entry at the apical plasma membrane, decays rapidly within the clear zone of the pollen tube and does not result in the evident propagation of a wave.

Simultaneous Measurement of Growth and the Extracellular Tip-Directed Ca^{2+}_o Influx

When it comes to interpreting extracellular ion currents, an unusual problem faces those working on cells with a wall; it is not clear whether the destination of the moving ions is the wall or the protoplast. Because the wall surrounds the protoplast entirely, any ions that move through the plasma membrane must first pass through the cell wall, and the wall itself may constitute an ion "sink" or "source." Thus, unlike animal cells, in any cell type with a wall, an extracellular current of a given ion does not necessarily mean that there is flux across the plasma membrane. We use the term "influx" to describe an inward movement of the ion relative to the cell from the external solution. However, when using the vibrating probe, we are unable to distinguish between ions moving into the wall alone and ions moving through the wall and then through the plasma membrane.

Extracellular measurements using an ion-selective vibrating electrode have revealed that an inwardly directed flux of Ca^{2+}_o occurs at the tip of growing pollen tubes (Kühtreiber and Jaffe, 1990). More recent work indicates that treatments that inhibit growth and dissipate the tip-focused $[Ca^{2+}]_i$ gradient, for example, BAPTA buffer injection, caffeine application, and mild thermal shock, also greatly reduce the Ca^{2+}_o current at the tip (Pierson et al., 1994, 1996). Exploring this matter further now reveals that the inward Ca^{2+}_o current exhibits oscillatory behavior.

Ca^{2+}_o fluxes were measured in LCLB medium. Figures 3A

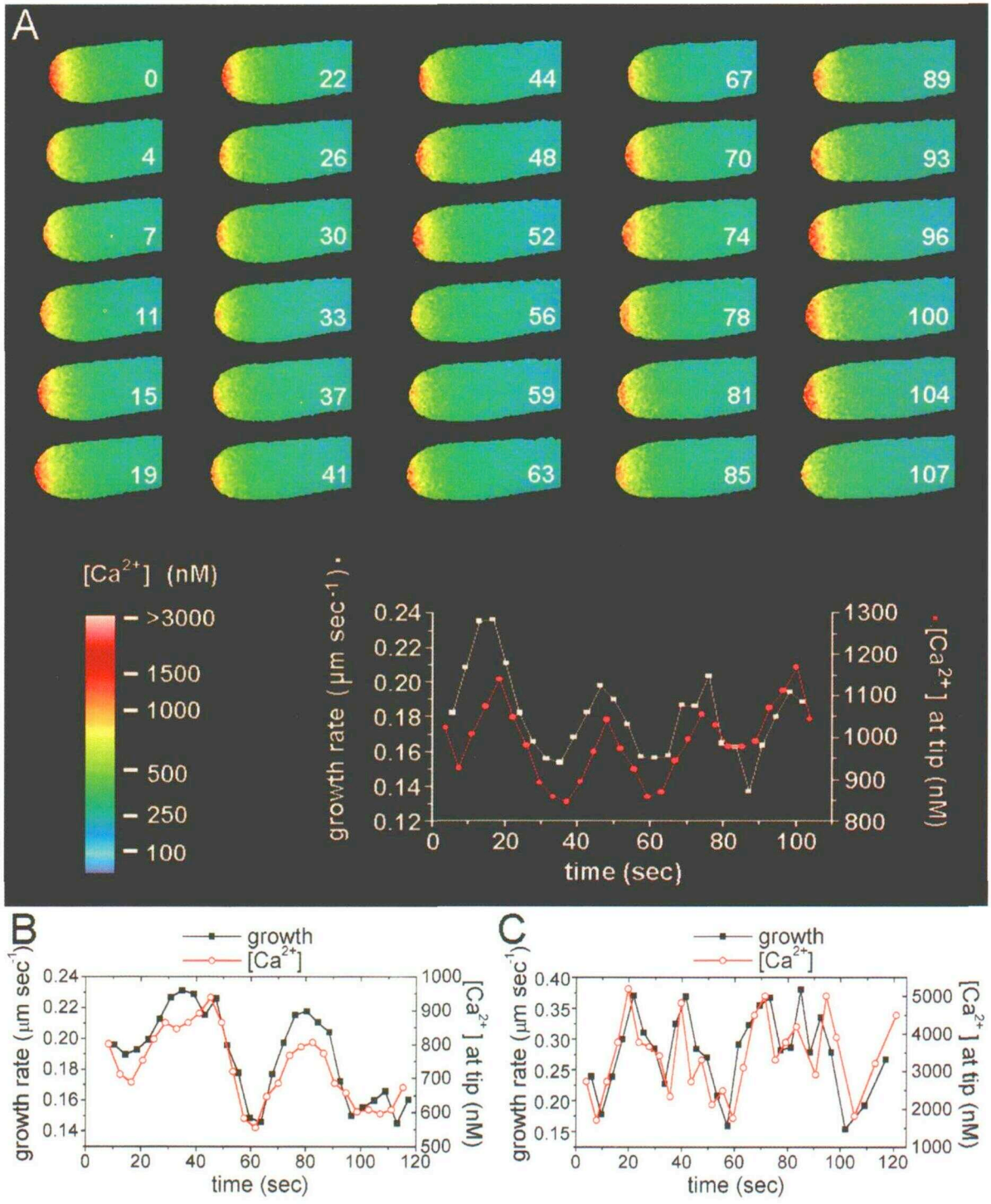

Figure 1. Pollen Tube Growth and Free Calcium at the Tip Oscillate in Phase.

(A) Pseudocolor ratio images of a growing pollen tube in regular medium loaded with fura-2–dextran. Time in seconds is given on each image (images were taken ~3.7 sec apart). Growth rate and $[Ca^{2+}]_i$ in the same tube are plotted as a function of time.

(B) Time course for another pollen tube in regular medium showing oscillations in growth (black) and tip $[Ca^{2+}]_i$ (red).

(C) Growth and tip $[Ca^{2+}]_i$ as given for **(B)** but in LCLB medium.

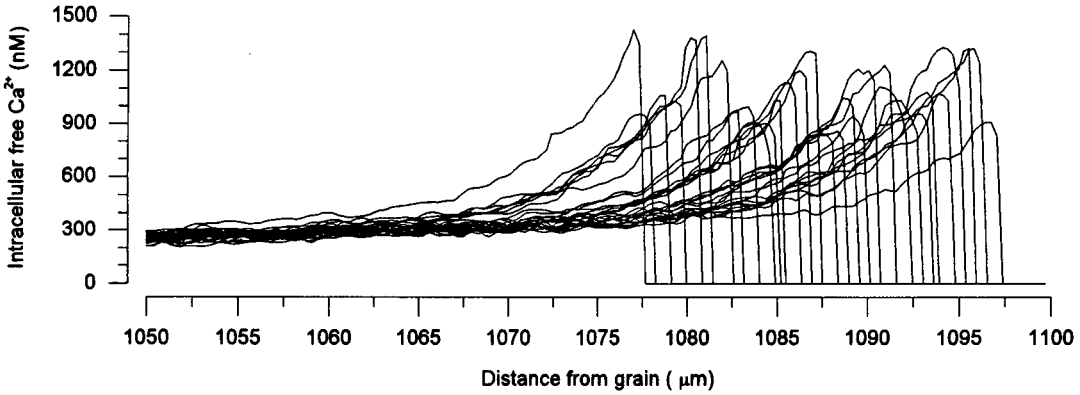

Figure 2. Nested Profiles of $[Ca^{2+}]_i$ Oscillation.

Line scan profiles of the 30 pollen tube images shown in Figure 1A are depicted here. As the tube grows, the tip gradient advances. Variations in the spacing of the profiles indicate changes in the growth rate between images. The change in the gradient occurs right at the tip, with each profile fitting the curve for an exponential decay.

and 3B demonstrate that the $Ca^{2+}{}_o$ influx at the tip of lily pollen tubes oscillates, with periods similar to the oscillations of the growth rates. In contrast to intracellular measurements, the two oscillations did not appear to be in phase but rather were offset from each other. As measurements were taken and the tube grew, it was necessary to make small adjustments (<0.5 μm) to the position of the probe so that it did not touch the growing tip. This movement of the probe did not produce any significant artifact (Figure 3B). The magnitude of fluxes measured at the tip of

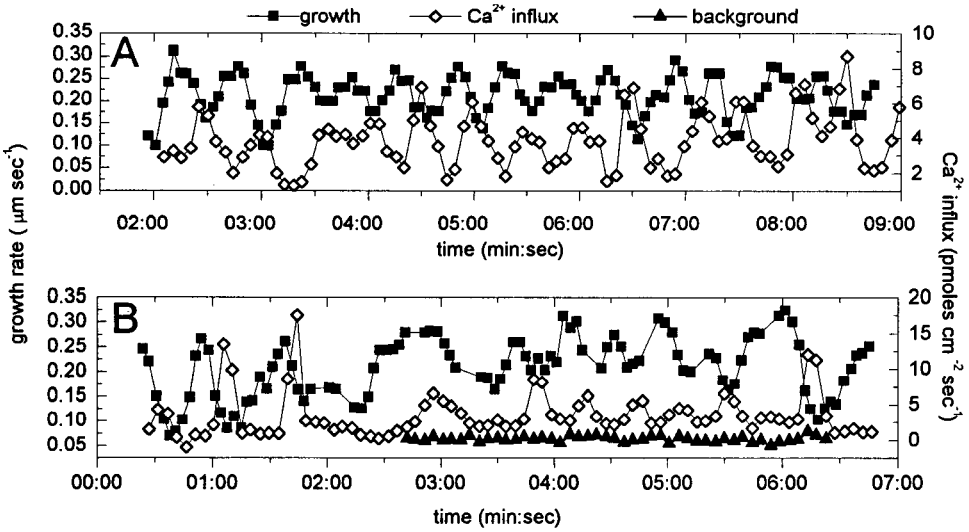

Figure 3. Calcium Influx Oscillates Out of Phase with the Growth Rate.

Two examples of pollen tube growth (black squares) and $Ca^{2+}{}_o$ influx (open diamonds) at the tip, measured with the Ca^{2+}-selective vibrating probe. Fluxes measured while making incremental movements of the probe at a distance of 80 μm from the tip (**[B]**, triangles) showed that such movements are not responsible for the oscillations in $Ca^{2+}{}_o$ flux observed when the probe is moved in the same manner close to the tip.

(A) Simultaneous measurements of pollen tube growth and $Ca^{2+}{}_o$ influx show that both oscillate with similar periodicity.

(B) Shown is a recording of pollen tube growth and $Ca^{2+}{}_o$ influx in which the oscillations are not regular, making it clear that fluctuations in the growth rate precede similar changes in the $Ca^{2+}{}_o$ influx.

the tube was similar to the magnitude of those measured previously by Pierson et al. (1994).

Phase Relations of Growth, the Tip-Focused $[Ca^{2+}]_i$ Gradient, and Ca^{2+}_o Influx

We used cross-correlation analysis to quantify the phase relations of growth, the $[Ca^{2+}]_i$ gradient, and Ca^{2+}_o influx. Figure 4 shows that the cross-correlation between growth and $[Ca^{2+}]_i$ is maximal with zero offset, indicating that the growth rate and $[Ca^{2+}]_i$ oscillate in phase. In contrast, the Ca^{2+}_o influx is most strongly correlated with growth when the influx curves are out of phase 10 to 13 sec with respect to growth. A strength of the cross-correlation analysis resides in the use of all of the available data to estimate the correlation coefficient for every offset applied to the data sets. In such an analysis, the presence of irregularities in the periodicity and amplitudes of the oscillations strengthens the correlation coefficient at one offset only; if the oscillations and amplitudes were perfectly regular, there would be no way of determining which oscillation was leading and which was following. Indeed, by inspection alone, it became clear that irregularities in the growth oscillations are always followed by similar irregularities in the Ca^{2+}_o influx oscillations. For example, in Figure 3B, the first two complete growth oscillations shown are large and slightly precede correspondingly large oscillations in Ca^{2+}_o influx. The third complete growth peak, which is broad, is then followed by a similarly broad Ca^{2+}_o influx peak. After this, smaller oscillations in both growth and Ca^{2+}_o current were observed, with the Ca^{2+}_o influx always slightly behind growth.

From cross-correlation analyses of each experiment, the median phase of $[Ca^{2+}]_i$ oscillations with respect to growth oscillations was −1.6 sec (n = 15; 95% confidence limits; −2.1 and +1.1) for tubes measured in either medium, confirming our observations that the two oscillations are essentially in phase. The median phase of the Ca^{2+}_o influx with respect to growth was +11 sec (n = 5; 95% confidence limits; +10.8 and +13.1), that is, peak growth precedes the peak Ca^{2+}_o influx by 11 sec. In tubes showing regularly spaced oscillations of growth and ion influx, the period was between 27 and 33 sec, and the calculated phase difference with respect to the measured period was 149 ± 4° (n = 3). Statistical analysis showed that the phases of the oscillations in $[Ca^{2+}]_i$ and Ca^{2+}_o flux with respect to growth oscillations are significantly different (Mann-Whitney test; P = 0.05). Therefore, we conclude both from inspection and from our cross-correlation analysis that the Ca^{2+}_o influx follows an increase in growth and the simultaneous increase in the $[Ca^{2+}]_i$ gradient.

Both autocorrelation and Fourier analyses show that in many cases, the period of oscillation for growth matches that of oscillations in either the $[Ca^{2+}]_i$ or the Ca^{2+}_o influx very well. However, we were not able to determine the phase relationship between oscillations by using Fourier analysis.

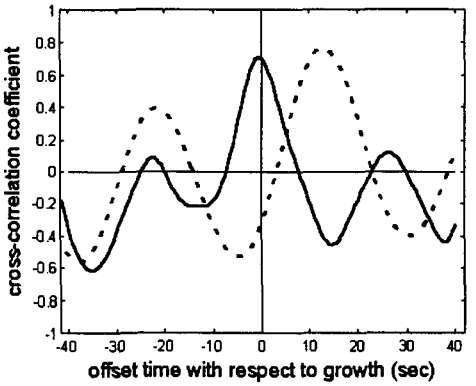

Figure 4. Cross-Correlation Analysis of Growth with the Tip-Focused $[Ca^{2+}]_i$ Gradient and Ca^{2+}_o Influx.

Each curve is the result of a cross-correlation analysis of a single experiment. Representative curves were chosen for the tip-focused $[Ca^{2+}]_i$ gradient (solid line) and Ca^{2+}_o influx at the tip (dotted line).

DISCUSSION

Our results show that both the tip-focused $[Ca^{2+}]_i$ gradient and the tip-directed Ca^{2+}_o influx oscillate with the same period as the growth rate in in vitro–cultured lily pollen tubes. However, the intracellular gradient oscillates in phase with growth, whereas the extracellular current is delayed by ~11 sec (Figure 5A). Given this difference, it is important to assess the accuracy of the methods used. The maximum offset of the vibrating probe data from its reported timing is 1.5 sec, and there is an uncertainty of 1 sec in synchronizing the video (growth) data with that from the probe. Thus, the total possible error in phase would be at most 2.5 sec. This by no means is sufficient to account for the 11-sec phase difference observed. In addition, the period of oscillation of the probe is 0.3 Hz, whereas the period of oscillation observed was ~10 times slower. Therefore, it is unlikely that we are observing an artifact from the oscillation of the probe. This conclusion is further confirmed by the lack of oscillations seen when the measurements were taken at a distance of 80 μm from the pollen tube, as shown in Figure 3B.

Is Ca^{2+}_o Influx Sufficient to Supply the $[Ca^{2+}]_i$ Gradient at the Tip?

The vibrating probe measured an oscillating Ca^{2+}_o influx of up to 20 pmol cm^{-2} sec^{-1} at the tip of growing pollen tubes in LCLB medium. The flux required to support the tip-focused $[Ca^{2+}]_i$ gradient was calculated using median-filtered line scans of ratio images of tubes growing in LCLB

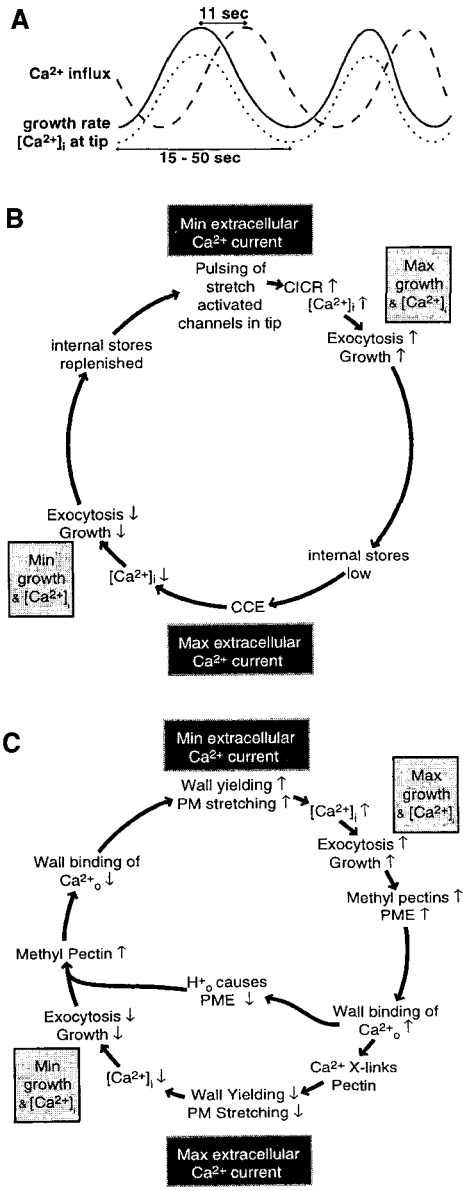

Figure 5. Schematic and Two Models for Oscillatory Growth in Pollen Tubes.

(A) Schematic showing the temporal relationship among oscillations in growth, $Ca^{2+}{}_o$ influx, and the $[Ca^{2+}]_i$ gradient.

(B) Internal stores model. Oscillation of growth and $[Ca^{2+}]_i$ could involve release of $Ca^{2+}{}_i$ from internal stores such as the ER or vesicles by calcium-induced calcium release (CICR). Stores could be refilled by capacitative calcium entry (CCE). See text for more detail.

(C) External stores model. The cell wall could act as a growth regulator, in which its rigidity controls the opening of stretch-activated channels in the plasma membrane (PM) and which in turn is self-regulating; pectin methylesterase (PME) acts, allowing Ca^{2+} to cross-link pectins. The binding of Ca^{2+} also releases H^+, lowering the pH of the wall space and inhibiting the activity of PME. See text for more detail.

Max, maximum; Min, minimum; X-links, cross-links.

medium. For pollen tubes in this medium, the characteristic distance (the distance over which the concentration falls to $^1/_e$ of the amplitude of the $[Ca^{2+}]_i$ oscillation) was ~6 μm. The relaxation time for $Ca^{2+}{}_i$ diffusion (the time it takes a component of the gradient to diffuse its characteristic distance) is calculated by τ = (characteristic distance)$^2/D \cdot$ (dimensions × 3), in which D is the diffusion coefficient for Ca^{2+} in the cytoplasm (10^{-7} cm^{-2} sec^{-1}; Thomas, 1982), and yields a value of 0.6 sec. Because this is much shorter than is the period of oscillation of the gradient (~30 sec), the equation used to describe steady state diffusion from one end of a cylinder could be applied (as done by Miller et al., 1992). The solution for the steady state spatial distribution of $Ca^{2+}{}_i$ at a distance x from the tip is $[Ca^{2+}]_i = B + A \exp[-x(\sqrt{}(p/D))]$, in which B is the basal level of $[Ca^{2+}]_i$, A is the amplitude of the $[Ca^{2+}]_i$ gradient (i.e., the difference between the maximum $[Ca^{2+}]_i$ and B), and p is the pumping capacity of Ca^{2+} extrusion from the cytoplasm. Applying Fick's law to this model and solving at $x = 0$ determines that flux at the tip is $A \cdot D(\sqrt{}(p/D))$. With A = 3000 nM, the calculated influx was 0.5 pmol cm^{-2} sec^{-1}, much smaller than the measured influx, which usually oscillated ~5 to 10 pmol cm^{-2} sec^{-1}. These calculations thus indicate that the extracellular influx is at least an order of magnitude greater than is the amount needed to support the observed intracellular apical gradient.

An increase in apical $[Ca^{2+}]_i$ could be the result of increased influx at the tip, reduced $Ca^{2+}{}_i$ extrusion from the cytoplasm, or release of Ca^{2+} from intracellular stores. For each of the five tubes grown in LCLB medium, the calculated influx was always greater for the image corresponding to fast growth than for the one corresponding to slow growth, whereas the characteristic distance did not consistently increase or decrease with the growth rate. The characteristic distance = $\sqrt{}(D/p)$, and because D is unlikely to change, it appears that p, the pumping capacity of the cytoplasm, does not change either. This is an indication that oscillations in the $[Ca^{2+}]_i$ gradient are not generated by changes in the activity of Ca^{2+} pumps. Basal levels of $Ca^{2+}{}_i$ remained constant as the magnitude of the tip gradient oscillated, further indicating that release of Ca^{2+} from intracellular stores throughout the pollen tube is not involved in producing the oscillation. However, localized release of Ca^{2+} from the endoplasmic reticulum (ER) at the extreme apex of the tube has not been eliminated as a possibility by this analysis, because this would be mathematically indistinguishable from a tip-focused influx from outside the cell.

Requirements of a Model

In attempting to understand these observations and explain their relationship to the process of pollen tube elongation, it seemed important to inspect closely the nature of the intracellular gradient. The ratiometric images shown in this study

and in previous studies (Pierson et al., 1994, 1996; Malhó et al., 1995) reveal that the high point of $[Ca^{2+}]_i$ resides immediately adjacent to the plasmalemma, supporting the conclusion that the ion is derived from influx across the plasma membrane. It is notable that only with ratiometric techniques is the true nature of the calcium gradient revealed; in images obtained with the single wavelength dye Calcium Green-1, the diminishing pathlength at the tip of the pollen tube prevents visualization of any calcium gradient (Franklin-Tong et al., 1996; Malhó et al., 1996) and use of Calcium Green–dextran causes the highest $[Ca^{2+}]_i$ to appear to be located in the middle of the clear zone (Messerli and Robinson, 1997) rather than at the very tip. Further support for the idea that the gradient derives from influx comes from observations of radioactive calcium accumulation in the tip of growing pollen tubes (Jaffe et al., 1975) and the finding that both the gradient and growth are blocked by lanthanides (Malhó et al., 1994, 1995; Messerli and Robinson, 1997), which are known to act at the plasma membrane and not to enter the cell. Additionally, manganese in the culture medium quenches the dye and the apparent tip-focused gradient as a function of its entry into the pollen tube (Malhó et al., 1995).

Whereas these observations all indicate that calcium entry across the plasmalemma is involved in the formation and maintenance of the tip-focused $[Ca^{2+}]_i$ gradient, our data from the vibrating probe clearly indicate that the peak influx does not occur synchronously with the peak of the internal gradient but rather follows it by ~11 sec. The observed phase difference between the oscillations of $[Ca^{2+}]_i$ and the $Ca^{2+}{}_o$ inward-directed flux necessitates the existence of some kind of storage compartment for the entering calcium. Furthermore, because the temporal pattern of fluctuations in the $[Ca^{2+}]_i$ gradient seems to predict the pattern of inward $Ca^{2+}{}_o$ current 11 sec later, the filling of the storage compartment also must be dependent on the activity of the $[Ca^{2+}]_i$ gradient. We propose two possible mechanisms that could account for the observed 11-sec time delay between the peak of the $[Ca^{2+}]_i$ gradient and the peak influx of $Ca^{2+}{}_o$ at the tip; the first invokes internal Ca^{2+} stores, such as the ER, and the second involves external Ca^{2+} stores, the cell wall. A third model also could be generated by combining both models into a single scheme.

Internal Stores Model

In the first model (Figure 5B), brief opening of stretch-activated Ca^{2+} channels allows entry of a small amount of Ca^{2+}, which triggers calcium-induced calcium release (CICR) from internal stores, increasing the $[Ca^{2+}]_i$ gradient. Elevated $[Ca^{2+}]_i$ at the tip promotes vesicle exocytosis and hence cell elongation (Zorec and Tester, 1992; Battey and Blackbourn, 1993). Capacitative calcium entry (CCE; Putney, 1990; Berridge, 1995) across the plasma membrane, so called because discharge promotes refilling of the store, could start to recharge internal stores almost as soon as calcium is released. However, this $Ca^{2+}{}_o$ influx may peak 11 sec after maximum $[Ca^{2+}]_i$ at the tip, thus accounting for the observed phase delay, but only if far more Ca^{2+} is taken up than is released.

This model is similar to signaling in animal cells in which the ER is the primary store of Ca^{2+}; indeed, in exocrine cells from the avian salt gland, entry of Ca^{2+} across the plasma membrane occurs some 20 to 30 sec after the peak of Ca^{2+} release from internal stores (Shuttleworth, 1994). As $Ca^{2+}{}_i$ is continually sequestered from the cytoplasm, the $[Ca^{2+}]_i$ gradient decreases; as a result, the rates of exocytosis and growth also decline. The cycle may be started again by rhythmic cooperative opening of stretch-activated Ca^{2+} channels at the tip. For example, Ding and Pickard (1993) have shown an endogenous pulsing of calcium currents every 10 to 15 sec in onion cell epidermal protoplast–attached patches with applied suction of 3.7 kPa. It is feasible that a similar, periodically pulsing channel could operate in pollen tubes where the turgor pressure is 100 times higher (Benkert et al., 1997). Because the temporal pattern of the gradient is determined by the pattern of CICR, refilling of internal stores by CCE could be predicted by the gradient, as is observed. Inositol phosphates may be involved in facilitating CICR, because Franklin-Tong et al. (1996) have shown that pollen tubes contain a Ca^{2+}-activated phosphoinositide-specific phospholipase C activity and that uncaging of inositol (1,4,5)-trisphosphate can induce release of Ca^{2+}. Trewavas and Malhó (1997) have proposed a model for control of pollen tube reorientation involving inositol (1,4,5)-trisphosphate and CICR, but the model cannot explain the continuous nature of oscillations in growth, $[Ca^{2+}]_i$ at the tip, and $Ca^{2+}{}_o$ influx.

Despite its attractiveness, there are certain difficulties with the internal stores model that should be noted. Although ER is present in the apical clear zone, it is not especially concentrated in this region (Lancelle and Hepler, 1992) or closely appressed to the plasmalemma in such a way that would seem to facilitate formation of such a sharply tip-focused gradient. It is also notable that although CICR causes $[Ca^{2+}]_i$ gradients to spread in a wavelike manner through the cytoplasm in many situations, such waves are not seen under normal growth conditions in the tip region of the growing pollen tube. Movement of Ca^{2+} through ER "tunnels" to the tip region, as seen in pancreatic acinar cells (Mogami et al., 1997), could conceivably produce the observed gradient without waves and allow recharging of the ER at a phase in the cycle in which ratio-imaging of the tip indicates a decline in $[Ca^{2+}]_i$. Vesicles, which are concentrated in the tip region, are also candidates for Ca^{2+} stores, but little is known of their ability to act in this capacity. Regardless of whether the chief store of Ca^{2+} is the ER or vesicles, the fact that the calculated influx of $Ca^{2+}{}_o$ required to produce the gradient is over an order of magnitude smaller than that measured with the vibrating probe indicates that the influx of $Ca^{2+}{}_o$ is doing more than supplying the intracellular tip-focused gradient and that an external store of calcium may be involved in pollen tube tip growth.

External Stores Model; the Cell Wall as Growth Regulator

The exponential decline of the gradient (as shown in Figure 2) is consistent with Ca^{2+} entry across the plasmalemma at the tip as the sole supply of the ion. If the elevation of $[Ca^{2+}]_i$ directly correlates with cell expansion, and if these ions are derived from transport across the plasmalemma, then the extracellular current could be delayed in phase by 11 sec if the dominant current represents flow of Ca^{2+}_o into the cell wall space. Periodic changes in the ion binding properties of the cell wall polymers could account for the observed oscillations in Ca^{2+}_o influx and in the mechanical properties of the wall that control growth (see Figure 5C).

An obvious wall polymer candidate would be pectin, which is the major component of the pollen tube cell wall at the tip (Heslop-Harrison, 1987) and which is thought to be secreted in a methylesterified state (Zhang and Staehelin, 1992). Pectin methylesterases (PMEs), which also are secreted (Quentin et al., 1997), would cleave the methylester groups, exposing anionic sites (a Ca^{2+} "sink") on the pectin polymer. Free Ca^{2+} in the cell wall cross-links pectins into the "egg-crate" configuration (Grant et al., 1973), which is likely to have a higher yield threshold than would unlinked pectin and therefore slow growth. The delay between growth and Ca^{2+}_o influx could well be the result of two phenomena: the chemical reaction time for PME to cleave the methylester groups, and the time required for Ca^{2+}_o to diffuse from the solution into the free space of the cell wall and from there to be incorporated into cross-linked pectins. Diffusion times through the cell wall are likely to be significantly slower than if the ions were diffusing through water (Canny, 1995). In addition, the concentration difference between the wall and the solution is far less than that for the cytoplasm compared with the cell wall.

Conversion of methylated pectins to their acidic form also creates binding sites for protons, which, in contrast to Ca^{2+}, would be expected to have a loosening effect on the cell wall (Cassab and Varner, 1988). Incoming Ca^{2+} displaces H^+ bound to acidic pectins, decreasing wall pH, which could deactivate PME, an enzyme whose activity declines sharply at lower pH (Moustacas et al., 1986). This deactivation would mean that given continuous exocytosis, the proportion of esterified pectin would increase as the Ca^{2+} cross-linked pectin is pushed out of the tip zone, resulting in a lower yield threshold. The ensuing stretching of the plasmalemma at the tip could open stretch-activated Ca^{2+} channels at the tip, allowing Ca^{2+} ions to enter. The diffusion of Ca^{2+} into the cytoplasm would appear to be simultaneous with growth, because the concentration difference across the plasmalemma is great, with the wall constituting an almost infinite Ca^{2+} source. In this model, the intracellular gradient determines the rate of deposition of pectins and PME, with the latter controlling the rate of production of anionic binding sites for Ca^{2+} on pectins and thus controlling the rate of Ca^{2+} influx. Because the calculated Ca^{2+}_o influx required to support the apical gradient is small and close to the limit of resolution of the ion-selective vibrating probe, the measured influx would be sufficient to account for the flow of ions across the plasma membrane, even at the troughs of the Ca^{2+}_o influx oscillation.

Some recent results provide support for this model. Studies with tobacco and other species indicate that in vitro–cultured pollen tubes exhibit pulsatory growth in which periods of very slow cell elongation are punctuated by brief periods of rapid forward extension (Tang et al., 1992; Pierson et al., 1995). Further analysis reveals that the cell wall is deposited in distinct bands that occur at periodic intervals (5 to 6 μm) along the length of the tube. Using selective antibodies that are specific for different cell wall components, Li et al. (1992, 1994) and Geitmann et al. (1995) found that these bands are enriched in acidic pectins and arabinogalactan proteins, with relatively less esterified pectin. In addition, these bands are deposited during periods of slow growth. Although lily pollen tubes normally exhibit uniform deposition of the wall components, they can be experimentally constrained into alternating periods of slow and fast growth (Li et al., 1996). Under these conditions, they too are seen to produce wall bands during periods of slow growth, which are positive for acidic pectins. These conclusions are supported by growth studies of other cell types. For example, in carrot suspension cells (McCann et al., 1993), salt-adapted tobacco cells (McCann et al., 1994), and maize coleoptiles (Kim and Carpita, 1992), slower growth is correlated with an increasing abundance of acidic pectins, whereas more rapid growth is correlated with a relative increase in esterified pectins.

Is Ca^{2+}_o Influx Sufficient to Supply the New Wall with Ca^{2+}?

A lily pollen tube growing at 10 μm min^{-1} with a diameter of 16 μm and wall thickness of 0.2 μm produces 1.6 μm^3 of cell wall every second. Assuming a specific gravity of 1 for the wall material, and assuming that the wall is 60% water (Grignon and Sentenac, 1991), this is equivalent to 640 fg sec^{-1}. The pollen tube is a single cell in which, due to tip growth, the wall is young at the tip but matures as it is pushed out to the flanks of the tube. Goldberg et al. (1986) showed that the Ca^{2+} content of pectins in cell walls extracted from mung bean hypocotyl increases as cells mature (80 μmol g^{-1} dry weight of cell wall in young tissue compared with 122.5 μmol g^{-1} in mature tissue), correlating with increasing proportions of pectins with a low degree of esterification. Movement of Ca^{2+} into the wall is required to supply the extra Ca^{2+} required as the pollen tube cell wall matures, and if it were to occur through a circular patch of cell wall at the tip, with a diameter of 10 μm, then the flux would be 35 pmol cm^{-2} sec^{-1}. This figure is in very good agreement with what we measure with the vibrating probe, especially considering that the efficiency of the Ca^{2+} selec-

tive probe is not likely to exceed 50%, resulting in underestimation of the real flux. We consider this strong evidence that the Ca^{2+} binding properties of the cell wall play an integral role in tip growth of lily pollen tubes.

Conclusions

Calculations show that there is sufficient influx of $Ca^{2+}{}_o$ at the tip to allow both entry of $Ca^{2+}{}_o$ into the protoplast at the tip to support the $[Ca^{2+}]_i$ gradient and extensive binding of $Ca^{2+}{}_o$ to unesterified pectins in the cell wall. Further work is required to determine whether internal stores are involved in producing the tip gradient.

The oscillatory nature of growth is not unique to pollen tubes. Remarkably similar oscillations have been described previously in several different fungal hyphae that extend by tip growth (López-Franco et al., 1994). Stretch-activated Ca^{2+} channels have been found at growing hyphal tips of fungal species (Garrill et al., 1992). These are also reported to have a tip-focused $[Ca^{2+}]_i$ gradient (Garrill et al., 1993; Levina et al., 1995; Hyde and Heath, 1997), and future studies are likely to reveal that it also oscillates. The contribution of Ca^{2+} to tip growth is supported by the finding of tip-directed currents and focused gradients in other systems, including root hairs (Schiefelbein et al., 1992; Felle and Hepler, 1997) and Fucus rhizoids (Brownlee and Wood, 1986; Taylor et al., 1996); however, in these systems, much less is known about the growth oscillations. Nevertheless, it is reasonable to imagine that oscillatory growth and its underlying causes are general properties of all tip-growing cells. The pollen tube, however, is favored for continued studies on tip growth because of its accessibility, extremely rapid growth, apparently simple cell wall structure, and ease of experimental manipulation. Understanding this simplified system may provide vital clues in deciphering the general mechanism of plant cell elongation.

METHODS

Pollen Culture

Pollen grains of *Lilium longiflorum* were germinated in one of two germination media containing 10% sucrose. Regular germination medium was the same as that used in our previous studies (Miller et al., 1992; Pierson et al., 1994, 1996), consisting of 0.1 mM KCl, 0.1 mM $CaCl_2$, 1.6 mM H_3BO_3, and 15.0 mM Mes, pH 5.5. The low-Ca^{2+}, low-buffer medium (LCLB) was devised for use with the extracellular Ca^{2+}-selective vibrating probe and consisted of 1.0 mM KCl, 0.05 mM $CaCl_2$, 1.6 mM H_3BO_3, and 1.0 mM Mes, pH 6.0. Once germinated, pollen tubes grown in either regular medium or LCLB were fixed to a coverslip forming the bottom of a microscope slide chamber with a thin layer of media supplemented with 1.2% low gelling point agarose (type VII; Sigma). When the agarose had gelled, the chamber was filled with medium. All measurements were made on tubes at least 700 μm in length, because these show regular growth oscillations (Pierson et al., 1996).

Ratiometric Imaging of Cytosolic Ca^{2+}

Pollen tubes were pressure-injected with 2.5 mg mL^{-1} or 5 mg mL^{-1} fura-2–dextran (10 kD; Molecular Probes, Eugene, OR) in 5 mM Hepes buffer, pH 7.0. We estimate that pressure injection adds ~1% to the cell volume, which would result in a cytoplasmic concentration of fura-2–dextran between 2.5 and 5 μM. Images were captured on a CCD camera (Photometrics, Ltd., Tucson, AZ) attached to a Nikon (Tokyo, Japan) inverted microscope at excitation wavelengths of 340 nm (Ca^{2+} dependent) and 360 nm (Ca^{2+} independent). Ratio images were calculated from background-subtracted images of the Ca^{2+}-dependent and Ca^{2+}-independent wavelengths (340:360 nm), and a threshold was applied such that areas containing little or no dye (low pixel intensity at 360 nm) were set to black. PMIS (GKR Computer Consulting, Boulder, CO) image acquisition software enabled us to acquire a 340:360 nm image pair from the CCD camera every 3 to 5 sec and to record the exact time at which each pair was taken. Ratio image and area average calculations were also performed using PMIS. Cytosolic $[Ca^{2+}]$ at the tip was calculated by taking the average of a 7 × 8 pixel (4.7 μm^2) area at the very tip of the pollen tube.

Extracellular Flux Measurements

A Ca^{2+}-selective vibrating electrode (Kühtreiber and Jaffe, 1990) was used to measure extracellular $Ca^{2+}{}_o$ currents at the tips of lily pollen tubes. Electrodes were pulled from 1.5-mm glass capillaries (model TW150-4; World Precision Instruments, Inc., Sarasota, FL) with an electrode puller (Sutter Flaming/Brown model P-97; Sutter Instrument Co., Novato, CA), and the tips were made hydrophobic by baking at 250°C for at least 2 hr, followed by exposure to dimethyl–dichlorosilane (Sigma D-3879) vapor at 250°C for 10 min and continued baking for at least 1 hr. Electrodes were backfilled with 100 mM $CaCl_2$ to a length of 15 mm from the tip, and then a 10- to 15-μm column of Ca^{2+}-selective liquid ion exchange cocktail (Fluka Chemie AG Ca^{2+} ionophore I, cocktail A, Buchs, Switzerland) was drawn into the tip of the electrode by application of suction to the butt end of the pipette. An Ag/AgCl wire electrode holder (World Precision Instruments, Inc.) inserted in the back of the electrode established electrical contact with the bathing solution. The ground electrode was an Ag/AgCl half-cell (World Precision Instruments, Inc.) connected to the solution by a 0.5% agar bridge containing 3 M KCl. Signals were measured by a purpose-built electrometer (Applicable Electronics, West Yarmouth, MA). Electrode vibration and positioning were achieved with a three-dimensional positioner. Data acquisition, preliminary processing, and control of the stepper motor-driven positioner were done with the program 3DVIS (adapted by J.G. Kunkel from Version 6 of the program DVIS, described by Smith et al. [1994]).

The self-referencing vibrating probe oscillated at 0.3 Hz with an excursion of 10 μm, completing a whole cycle in just over 3 sec. At each position, the probe recorded 10 time "bins" of data. The first three bin averages at each position were discarded, allowing the probe to settle after its move, and the remaining seven were averaged. This settled average was then subtracted from each of the bins of data acquired at the next position of the probe; this subtraction represented the self-referencing feature of the probe (each position was referenced to the settled average of the last position). A rolling average was recorded and timed at the end of each bin. Each rolling

average included 14 self-referenced bin averages: the current bin plus the 13 preceding bins. Strictly speaking, each rolling average was statistically dependent on the preceding 13 and the next 13 rolling averages, by virtue of sharing bin averages.

Extracellular Ca^{2+} fluxes at the tip of a pollen tube were measured by positioning the electrode tip on the normal to the tangent at the very tip and setting the direction of vibration to be parallel to the long axis of the pollen tube. Thus, the probe measured the voltage at two points: close to the tip and 10 μm farther away.

Germinated pollen tubes were fixed to the coverslip base of a microscope slide chamber, as described above. The whole setup was built around an inverted microscope (model IM35; Carl Zeiss, Inc., Thornwood, NY), with video camera attached, and connected to a video recorder. Cells selected for measurement were 800 to 2000 μm in length and were growing parallel to the base of the chamber. The growth of the tube was recorded on videotape.

Growth Measurements

The growth rate of pollen tubes was measured either from videotape, in the case of ion flux experiments, or from the 360-nm images obtained in the process of imaging $[Ca^{2+}]_i$. Frames were captured from videotape every 2 to 4 sec, and the position of the tip as well as the time were recorded for each frame. From these position and time data, growth rates were calculated. The rate calculated from two adjacent frames was assigned to a time midway between them. Growth data were aligned with $Ca^{2+}{}_o$ flux data by a synchronizing light signal that appeared on the video and on the electronic notebook part of 3DVIS.

Background-subtracted images taken at 360 nm (Ca^{2+}-independent) excitation were used to determine the growth rate of lily pollen tubes in $[Ca^{2+}]_i$-imaging experiments. Because the path length of the dye increases farther back from the very tip, a line scan of this image has a sigmoidal shape. Corresponding positions on successive images were obtained by doing a Boltzman fit to the line scan and finding the x-coordinate of the midpoint of the sigmoid curve (analysis done on Origin from MicroCal Software, Inc., Northampton, MA). These position data were used to calculate the average growth rate between frames, and the rate was assigned to the time point midway between the two frames.

Phase Analysis

The phase relationship for growth, the $[Ca^{2+}]_i$ gradient, and $Ca^{2+}{}_o$ influx at the tip were investigated by cross-correlation analysis using custom Matlab (MathWorks, Inc., Natick, MA) scripts. All experiments consisted of growth data and ion data (either $[Ca^{2+}]_i$ measurements from fura-2–dextran ratio images or flux measurements of $Ca^{2+}{}_o$ made with the vibrating probe). Cross-correlation analysis consisted of splining both data sets with a common equispaced time basis and then calculating the standard product moment correlation coefficient as the data sets were incrementally offset from each other.

The standard product moment correlation coefficient (r) is defined by the following equation:

$$r = \frac{S_{xy}}{\sqrt{S_{xx}S_{yy}}}$$

in which the following summations of x and y are performed from $i = 1, \ldots, n$.

$$S_{xx} = \sum_i [(x_i - \bar{x})^2]$$

$$S_{yy} = \sum_i [(y_i - \bar{y})^2]$$

$$S_{xy} = \sum_i [(x_i - \bar{x}) \times (y_i - \bar{y})]$$

Time series cross-correlation analysis was performed by starting with a simple correlation calculation of the two data sets, X and Y, which produced a correlation with a zero offset. The procedure continued by sequentially offsetting the two splined sets of data with common unit intervals by a 1-unit interval and performing the correlation analysis again. This produced a cross-correlation with offset $+1$ or -1, depending on the direction in which the moving data set was offset. The second cross-correlation then had $(n - 1)$ elements, because the offset had discarded one unmatched data element. Repeating the correlation of the data sets at progressively increasing offsets yielded cross-correlation curves such as the ones shown in Figure 4. Although this analysis involved the use of nonindependent data several times over in the calculations, we are confident of the results obtained, because we consistently observed similar phase relationships for similar experimental situations. Further, Fourier analysis of the data also indicated that the periodicity of the growth matched that of either the $[Ca^{2+}]_i$ tip gradient or the $Ca^{2+}{}_o$ influx.

The correlation coefficient calculated for each offset value is a measure of how well the data sets correlate with each other at this position. A correlation coefficient of 1 means that the data sets are identical and exactly superimposed upon each other at this position. For example, in our case, growth varied from slow to fast, $Ca^{2+}{}_o$ influx varied from near zero to high, and the tip-focused $[Ca^{2+}]_i$ gradient varied from low to high. A correlation coefficient of 1 between growth and $[Ca^{2+}]_i$ at the tip means that fast growth is correlated perfectly with the steepest $Ca^{2+}{}_i$ gradient and, in the same data, that slow growth is correlated with the least steep gradient. Correspondingly, a correlation coefficient of -1 would indicate that fast growth is correlated perfectly with the least steep $[Ca^{2+}]_i$ gradient and, in the same data, that slow growth is perfectly correlated with the steepest $[Ca^{2+}]_i$ gradient. Thus, the time offset between the two data sets yielding the largest absolute value of the correlation coefficient gives the phase relationship between the two data sets.

ACKNOWLEDGMENTS

We thank all of our colleagues in the laboratory for helpful discussions. Special thanks to Drs. Stéphane Roy and Martin Canny for valuable discussions on properties of the cell wall and to Drs. Dave Gross and Ian Clarke for assistance with mathematical modeling. We are indebted to our two anonymous reviewers, whose insightful comments resulted in a much improved final version of the manuscript. We also thank Alan Shipley for the generous donation of equipment to the Vibrating Probe Facility (University of Massachusetts, Amherst). J.A.F. received personal fellowships from the Fulbright Foundation, Luso-American Foundation for Development, Calouste Glubenkian Foundation, and the University of Lisbon. This project was supported by National Science Foundation Grant No. MCB-96-01087 to P.K.H.

Received June 27, 1997; accepted September 8, 1997.

REFERENCES

Barnabás, B., and Fridvalszky, L. (1984). Adhesion and germination of differently treated maize pollen grains on the stigma. Acta Bot. Hung. **30,** 329–332.

Battey, N.H., and Blackbourn, H.D. (1993). The control of exocytosis in plant cells. New Phytol. **125,** 307–338.

Benkert, R., Obermeyer, G., and Bentrup, F.-W. (1997). The turgor pressure of growing lily pollen tubes. Protoplasma **198,** 1–8.

Berridge, M.J. (1995). Capacitative calcium entry. Biochem. J. **312,** 1–11.

Brownlee, C., and Wood, J.W. (1986). A gradient of cytosolic free calcium in growing rhizoid cells of *Fucus serratus.* Nature **320,** 624–626.

Canny, M.J. (1995). Apoplastic water and solute movement: New rules for an old space. Annu. Rev. Plant Physiol. Plant Mol. Biol. **46,** 215–236.

Cassab, G.I., and Varner, J.E. (1988). Cell wall proteins. Annu. Rev. Plant Physiol. Plant Mol. Biol. **39,** 321–352.

Ding, J.P., and Pickard, B.G. (1993). Mechanosensory calcium-selective cation channels in epidermal cells. Plant Cell **3,** 83–110.

Felle, H.H., and Hepler, P.K. (1997). The cytosolic Ca^{2+} concentration gradient of *Sinapis alba* root hairs as revealed by Ca^{2+}-selective microelectrode tests and fura–dextran ratio imaging. Plant Physiol. **114,** 39–45.

Franklin-Tong, V.E., Drøbak, B.K., Allan, A.C., Watkins, P.A.C., and Trewavas, A.J. (1996). Growth of pollen tubes of *Papaver rhoeas* is regulated by a slow-moving calcium wave propagated by inositol 1,4,5-trisphosphate. Plant Cell **8,** 1305–1421.

Garrill, A., Lew, R.R., and Heath, I.B. (1992). Stretch-activated Ca^{2+} and Ca^{2+}-activated K^+ channels in the hyphal tip plasma membrane of the oomycete *Saprolegnia ferax.* J. Cell Sci. **101,** 721–730.

Garrill, A., Jackson, S.L., Lew, R.R., and Heath, I.B. (1993). Ion channel activity and tip growth: Tip-localized stretch-activated channels generate an essential Ca^{2+} gradient in the oomycete *Saprolegnia ferax.* Eur. J. Cell Biol. **60,** 358–365.

Geitmann, A., Li, Y.Q., and Cresti, M. (1995). Ultrastructural immunolocalization of periodic pectin deposition in the cell wall of *Nicotiana tabacum* pollen tubes. Protoplasma **187,** 172–181.

Goldberg, R., Morvan, C., and Roland, J.C. (1986). Composition, properties and localisation of pectins in young and mature cells of the mung bean hypocotyl. Plant Cell Physiol. **27,** 417–429.

Grant, G.T., Morris, E.R., Rees, D.A., Smith, P.J.C., and Thom, D. (1973). Biological interactions between polysaccharides and divalent cations: The egg-box model. FEBS Lett. **32,** 195–198.

Grignon, C., and Sentenac, H. (1991). pH and ionic conditions in the apoplast. Annu. Rev. Plant Physiol. Plant Mol. Biol. **42,** 103–128.

Hepler, P.K. (1997). Tip growth in pollen tubes: Calcium leads the way. Trends Plant Sci. **2,** 79–80.

Hepler, P.K., Holdaway-Clarke, T.L., Hackett, G., Lancelle, S.A., and Kunkel, J. (1997). Exocytosis in pollen tubes: Regulation by calcium. J. Exp. Bot. **48** (suppl.), 4.

Heslop-Harrison, J. (1987). Pollen germination and pollen tube growth. Int. Rev. Cytol. **107,** 1–78.

Hyde, G.J., and Heath, I.B. (1997). Ca^{2+} gradients in hyphae and branches of *Saprolegnia ferax.* Fungal Genet. Biol. **21,** 238–251.

Jaffe, L.A., Weisenseel, M.H., and Jaffe, L.F. (1975). Calcium accumulations within the growing tips of pollen tubes. J. Cell Biol. **67,** 488–492.

Kim, J.B., and Carpita, N.C. (1992). Changes in esterification of the uronic acid groups of the cell wall polysaccharides during elongation of maize coleoptiles. Plant Physiol. **98,** 646–653.

Kühtreiber, W.M., and Jaffe, L.F. (1990). Detection of extracellular calcium gradients with a calcium-specific vibrating electrode. J. Cell Biol. **110,** 1565–1573.

Lancelle, S.A., and Hepler, P.K. (1992). Ultrastructure of freeze-substituted pollen tubes of *Lilium longiflorum.* Protoplasma **167,** 215–230.

Levina, N.N., Lew, R.R., Hyde, G.J., and Heath, B. (1995). The roles of Ca^{2+} and plasma membrane ion channels in hyphal tip growth of *Neurospora crassa.* J. Cell Sci. **108,** 3405–3417.

Li, Y.Q., Bruun, L., Pierson, E.S., and Cresti, M. (1992). Periodic deposition of arabinogalactan epitopes in the cell wall of pollen tubes of *Nicotiana tabacum* L. Planta **188,** 532–538.

Li, Y.Q., Chen, F., Linskens, H.F., and Cresti, M. (1994). Distribution of unesterified and esterified pectins in cell walls of pollen tubes of flowering plants. Sex. Plant Reprod. **7,** 145–152.

Li, Y.Q., Zhang, H.Q., Pierson, E.S., Huang, F.Y., Linskens, H.F., Hepler, P.K., and Cresti, M. (1996). Enforced growth-rate fluctuation causes pectin ring formation in the cell wall of *Lilium longiflorum* pollen tubes. Planta **200,** 41–49.

López-Franco, R., Bartnicki-Garcia, S., and Bracker, C.E. (1994). Pulsed growth of fungal hyphal tips. Proc. Natl. Acad. Sci. USA **91,** 12228–12232.

Malhó, R., and Trewavas, A.J. (1996). Localized apical increases of cytosolic free calcium control pollen tube orientation. Plant Cell **8,** 1935–1949.

Malhó, R., Read, N.D., Trewavas, A.J., and Pais, M.S. (1994). Role of cytosolic free calcium in the reorientation of pollen tube growth. Plant J. **5,** 331–341.

Malhó, R., Read, N.D., Trewavas, A.J., and Pais, M.S. (1995). Calcium channel activity during pollen tube growth and reorientation. Plant Cell **7,** 1173–1184.

Mascarenhas, J.P. (1993). Molecular mechanisms of pollen tube growth and differentiation. Plant Cell **5,** 1303–1314.

McCann, M.C., Stacey, N.J., Wilson, R., and Roberts, K. (1993). Orientation of macromolecules in the walls of elongating carrot cells. J. Cell Sci. **106,** 1347–1356.

McCann, M.C., Shi, J., Roberts, K., and Carpita, N.C. (1994). Changes in pectin structure and localization during the growth of unadapted and NaCl-adapted tobacco cells. Plant J. **5,** 773–785.

Messerli, M., and Robinson, K.R. (1997). Tip localized Ca^{2+} pulses are coincident with peak pulsatile growth rates in pollen tubes of *Lilium longiflorum.* J. Cell Sci. **110,** 1269–1278.

Miller, D.D., Callaham, D.A., Gross, D.J., and Hepler, P.K. (1992). Free Ca^{2+} gradient in growing pollen tubes of *Lilium.* J. Cell Sci. **101,** 7–12.

Mogami, H., Nakano, K., Tepikin, A.V., and Petersen, O.H. (1997). Ca^{2+} flow via tunnels in polarized cells: Recharging of apical Ca^{2+} stores by focal Ca^{2+} entry through basal membrane patch. Cell **88,** 49–55.

Moustacas, A.M., Nari, J., Diamantidis, G., Noat, G., Crasnier, M., Borel, M., and Ricard, J. (1986). Electrostatic effects and the dynamics of enzyme reactions at the surface of plant cells. 2. The role of pectin methyl esterase in the modulation of electrostatic effects in soybean cell walls. Eur. J. Biochem. **155,** 191–197.

Picton, J.M., and Steer, M.W. (1983). Evidence for the role of Ca^{2+} ions in tip extension in pollen tubes. Protoplasma **115,** 11–17.

Pierson, E.S., Miller, D.D., Callaham, D.A., Shipley, A.M., Rivers, B.A., Cresti, M., and Hepler, P.K. (1994). Pollen tube growth is coupled to the extracellular calcium ion flux and the intracellular calcium gradient: Effect of BAPTA-type buffers and hypertonic media. Plant Cell **6,** 1815–1828.

Pierson, E.S., Li, Y.Q., Zhang, G.Q., Willemse, M.T.M., Linskens, H.F., and Cresti, M. (1995). Pulsatory growth of pollen tubes: Investigation of a possible relationship with the periodic distribution of cell wall components. Acta Bot. Neerl. **44,** 121–128.

Pierson, E.S., Miller, D.D., Callaham, D.A., Van Aken, J., Hackett, G., and Hepler, P.K. (1996). Tip-localized calcium entry fluctuates during pollen tube growth. Dev. Biol. **174,** 160–173.

Putney, J.W. (1990). Capacitative calcium entry revisited. Cell Calcium **11,** 611–624.

Quentin, M., Jauneau, A., Morvan, O., Mareck, A., Gaffé, J., and Morvan, C. (1997). Immunolocalization of pectin methylesterases in the hypocotyl tissues of flax. Plant Physiol. Biochem. **35,** 475–482.

Rathore, K.S., Cork, J., and Robinson, K.R. (1991). A cytoplasmic gradient of Ca^{2+} is correlated with the growth of lily pollen tubes. Dev. Biol. **148,** 612–619.

Schiefelbein, J.W., Shipley, A., and Rowse, P. (1992). Calcium influx at the tip of growing root-hair cells of *Arabidopsis thaliana.* Planta **187,** 455–459.

Shuttleworth, T.J. (1994). Temporal relationships between Ca^{2+} store mobilization and Ca^{2+} entry in an exocrine cell. Cell Calcium **15,** 457–466.

Smith, P.J.S., Sanger, R.H., and Jaffe, L.F. (1994). The vibrating Ca^{2+} electrode: A new technique for detecting plasma membrane regions of Ca^{2+} influx and efflux. Methods Cell Biol. **40,** 115–134.

Tang, X.W., Liu, G.Q., Zheng, W.L., Wu, B.C., and Nie, D.T. (1992). Quantitative measurement of pollen tube growth and particle movement. Acta Bot. Sin. **34,** 893–898.

Taylor, A.R., Manison, N.F., Fernandez, C., Wood, J., and Brownlee, C. (1996). Spatial organization of calcium signaling involved in cell volume control in the Fucus rhizoid. Plant Cell **8,** 2015–2031.

Taylor, L.P., and Hepler, P.K. (1997). Pollen germination and tube growth. Annu. Rev. Plant Physiol. Plant Mol. Biol. **48,** 461–491.

Thomas, M.V. (1982). Techniques in Calcium Research. (New York: Academic Press).

Trewavas, A.J., and Malhó, R. (1997). Signal perception and transduction: The origin of the phenotype. Plant Cell **9,** 1181–1195.

Zhang, G.F., and Staehelin, L.A. (1992). Functional compartmentation of the Golgi apparatus of plant cells. Plant Physiol. **99,** 1070–1083.

Zorec, R., and Tester, M. (1992). Cytoplasmic calcium stimulates exocytosis in a plant secretory cell. Biophys. J. **63,** 864–867.